Structural and Functional Role of Helices I and II in Rhodopsin (I) IV.1

IV.1.1. A NOVEL INTERPLAY EVIDENCED BY MUTATIONS AT Gly-51 AND Gly-89 IN THE TRANSMEMBRANE DOMAIN

We started a detailed characterization of adRP mutants in the transmembrane region of rhodopsin with a 2-fold interest, (i) elucidation of the molecular mechanism of the disease and (ii) structural and functional information, from the study of these mutations that might be relevant to other members of the GPCR superfamily. The rhodopsin crystal structure together with the available biochemical data on rhodopsin mutants has shed more light into the molecular mechanism of RP associated with rhodopsin mutations [Garriga and Manyosa, 2002; Stojanovic and Hwa, 2002]. Previous studies show that conservative mutations in helix III at Leu-125 (site of the adRP mutation L125R) led to misfolding, and it was proposed that the folding of the intradiscal and transmembrane domains are coupled [Liu et al., 1996a, Garriga et al., 1996, Hwa et al., 1997]. These studies were further extended to dissect the effect of mutations at Leu-125 in the folding and function of rhodopsin [Andrés et al., 2001].

G51V and G89D naturally occurring adRP mutations were first reported in 1991 [Dryja et al., 1991; Sung et al., 1991a]. The G51A mutation was reported in 1993 [Macke et al., 1993]. A preliminary characterization of G51V [Sung et al., 1993] and G89D [Sung et al., 1991b] mutants together with other adRP mutations was carried out in 293S cell membranes. In another study these mutants were expressed in COS-1 cells and purified [Kaushal and Khorana, 1994]. Later, the mutants G51A, G51V, and G89D were studied in the context of the folding and packing of the transmembrane domain together with adRP mutations in the other helices of rhodopsin [Hwa et al., 1997]. These studies showed that G51V forms chromophore like wild-type rhodopsin (Wt), whereas G89D could only form it partially [Hwa et al., 1997]. We took these previous studies as a starting point for a detailed characterization of the helical environment of Gly-51 and Gly-89 in transmembrane helices I and II of rhodopsin by analyzing a series of mutants at these positions. In particular, one of

the questions we wanted to answer is what is the biochemical defect associated with Type I mutations (like G51V) which allow the protein to fold but still cause the disease. It was stated that the nature of this defect remained enigmatic [Sung et al., 1993].

Helices I and II have not received much attention in structural and functional studies because it was thought that they were not involved as major players in the process of rhodopsin activation. It seems clear, however, from the high degree of specificity in helix-helix interactions in rhodopsin that the wealth of information derived from mutagenesis studies is unraveling, making it necessary to address in detail the structural and functional effects of mutating amino acid residues of these helices.

In the present work, a series of mutations at the sites of the mutants associated with adRP, G51A, G51V (helix I), and G89D (helix II) have been constructed and characterized (Figure IV.1.1).

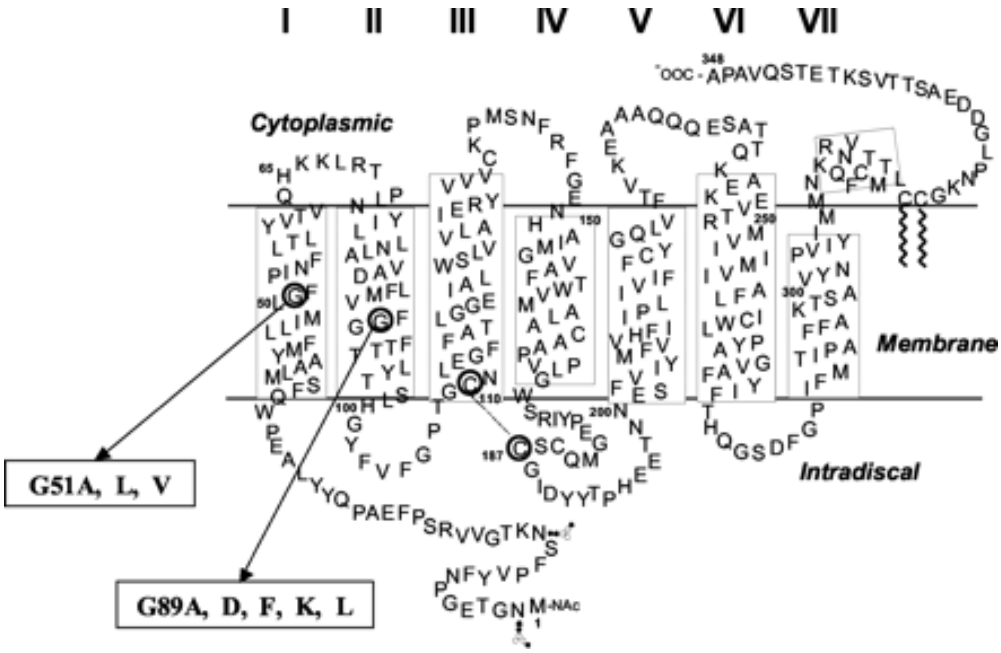

Fig. VI.1.1. A secondary structure model of bovine rhodopsin. The amino acids substituted in this work are *circled*, and the mutations studied are indicated. Cys-110 and Cys-187 form a disulfide bond (indicated by the *dashed line*), and Cys-322 and Cys-323 are palmitoylated. *Horizontal lines* approximately define the borders of the seven membrane-embedded helical segments (indicated by I–VII).

We find that mutations at position 51 are essentially affecting the optimal packing of the helices, with a clear destabilizing effect due to the size of the amino acid substitution. Furthermore, the G51V mutant is defective in signal transduction as a result of an unstable MetaII conformation. This suggests that mutations classified as Type I can be defective in dark state stability and in signal transduction. Mutations at position 89 are, in turn, more affected by the charge of the ionizable residues introduced in the transmembrane domain. The G89D mutant is also defective in transducin activation. Altered photointermediate formation, including faster MetaII decay and increased formation of other non-functional conformations of rhodopsin, like MetaIII, is proposed to be physiologically relevant for the mutations associated with adRP. Overall our results provide evidence for the presence of specific interhelical interactions, in the region delimited by helices I, II and VII in the transmembrane domain of rhodopsin, that are important for the stability and the function of the receptor.

IV.1.2. EXPRESSION AND CHARACTERIZATION OF MUTATIONS AT POSITION 51 IN HELIX I

Mutants G51A and G51V, associated with adRP, and the synthetic mutant G51L, expressed in transiently transfected COS-1 cells and purified by immunoaffinity chromatography with rho-1D4 antibody, showed an expression level similar to that of Wt. The SDS-PAGE pattern for these mutants was comparable with that of Wt, showing a main opsin band at around 40kDa and the absence of lower bands (not shown), usually associated with misfolded proteins [Liu et al., 1996a; Garriga et al., 1996; Ridge et al., 1995]. The reconstituted mutant rhodopsins eluted in 2mM NaH_2PO_4, pH 6.0, 0.05% DM (buffer A) formed normal chromophore and UV-visible absorption spectra like Wt (Figure IV.1.2), with A_{280}/A_{500} ratios of 1.6–1.7. The absorption spectra for the mutants showed small wavelength shifts in their corresponding visible absorption maxima. G51V had an absorbance maximum slightly red-shifted to 502nm, whereas G51L had it blue-shifted to 497nm (Table IV.1.I). Although the purified mutant proteins folded correctly to a conformation that was able to bind 11-*cis*-retinal-like Wt, thermal stability of the mutants in the dark was severely reduced (Table

IV.1.II). Furthermore, the secondary structure of the proteins was also less stable as measured by circular dichroism (data not shown).

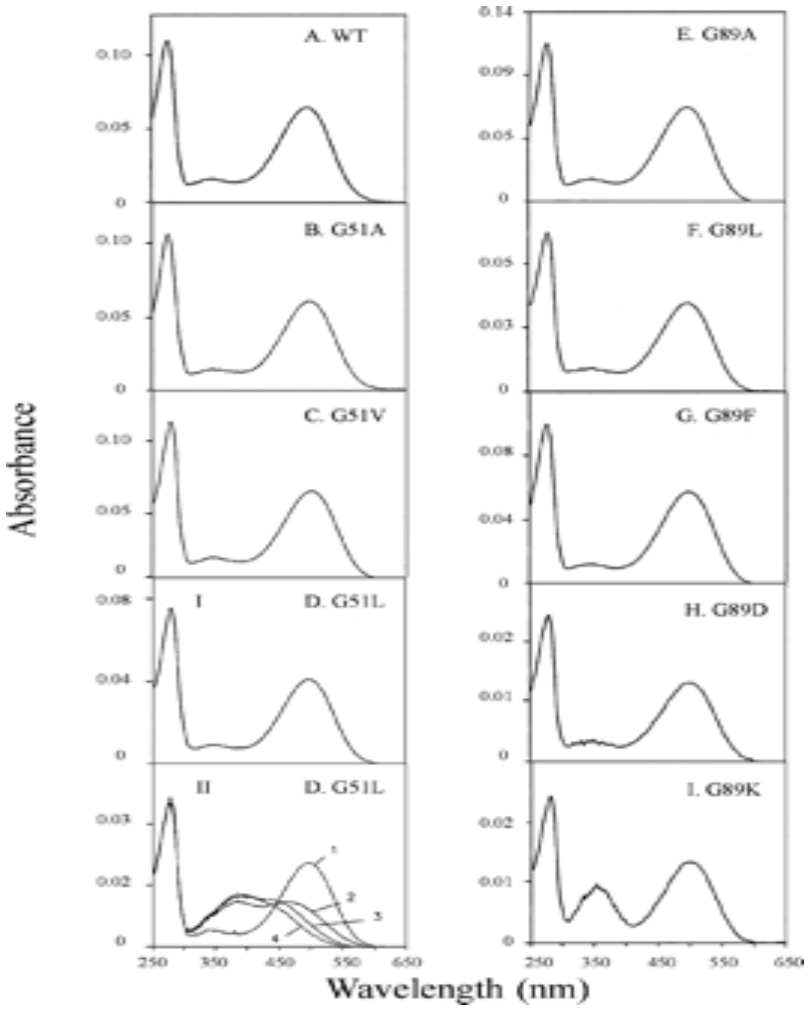

Fig IV.1.2. UV-visible absorption spectra of Wt and mutants at position 51 and 89. Mutant genes corresponding to Wt and mutant opsins were expressed in transiently transfected COS-1 cells, reconstituted with 11-*cis*-retinal, solubilized in DM, and immunopurified. The purified proteins were in buffer A. Spectra were recorded in the dark at 20°C. *A*, Wt from COS-1 cells; *B*, G51A (adRP) mutant; *C*, G51V (adRP) mutant; *D, I*, G51L mutant; D, *II*, G51L-photobleaching behavior. The sample was illuminated for different times with light of λ>495nm. *1*, non-illuminated dark sample; *2*, 10s; *3*, 30s; *4*, 1min. *E*, G89A; *F*, G89L mutant; *G*, G89F mutant; *H*, G89D (adRP) mutant; *I*, G89K mutant.

Rhodopsin	λ_{max} *nm*	$\varepsilon_{500\,nm}$ $M^{-1}\,cm^{-1}$
Wt(COS)	500	40,600
G51A	500	38,900
G51V	502	40,600
G51L	497	39,800
G89A	500	41,200
G89L	500	40,300
G89F	500	41,300
G89K	500, 350	30,900
G89D	500	39,100

Table IV.1.I. Absorption maxima and molar extinction coefficients of the Wt and the mutant rhodopsins

Protein	$t_{1/2}$ thermal bleaching *min*
Wt	54.6
G51A	32.2
G51V	2.6
G51L	<1.0

Table IV.1.II $t_{1/2}$ values for the thermal bleaching process of the Gly-51 mutants at 55°C in the dark

The photobleaching behavior of G51A mutant was normal, like that of the Wt (data not shown), but that of G51L was clearly altered (Figure IV.1.2, *panel D, II*). After 10s of illumination with light >495nm, in the case of mutant G51L, the 497nm species was not fully converted to the 380nm species. Instead, two bands of similar intensity were detected, one at 380nm and the other one at about 470nm (*trace 2* in *Panel D, II*, Figure IV.1.2). Further illumination for 30s or 1min (*traces 3* and *4* in *Panel D, II*, Figure IV.1.2) only caused a slight decrease of the 470nm band with a concomitant small increase in the 380nm band. A very similar behavior was previously seen for G51V [Hwa et al., 1997].

MetaII decay, as measured by fluorescence spectroscopy, was faster with increasing size of the amino acid side chain at position 51 (Figure IV.1.3). Thus, G51A and G51V decay curves could be fit to single exponential functions with $t^{1/2}$ of 23.2 and 15.7min, respectively (Table IV.1.III). G51L decay, however, could not be fit to a single exponential but to a double exponential function with a very fast component ($t^{1/2}$, 0.7min) and a slow component ($t^{1/2}$, 19.8min). MetaII decay was also measured for the rhodopsin mutant samples in 10mM Tris-HCl, pH 7.1, 100mM NaCl, 2mM MgCl2, and 0.012% DM (G_t assay buffer) (Table IV.1.III). Under these experimental conditions, $t^{1/2}$ for the decay of G51A was now slightly faster, 18.7min as compared with 23.2 min in buffer A. However, the decay for the G51V mutant could no longer be fit to a single exponential, and it had to be fit to a double exponential function, with two components, one very fast ($t^{1/2}$, 1.9min) and the other slow ($t^{1/2}$, 30.2min). G51L did not show any significant change in the MetaII decay values obtained in the G_t assay buffer.

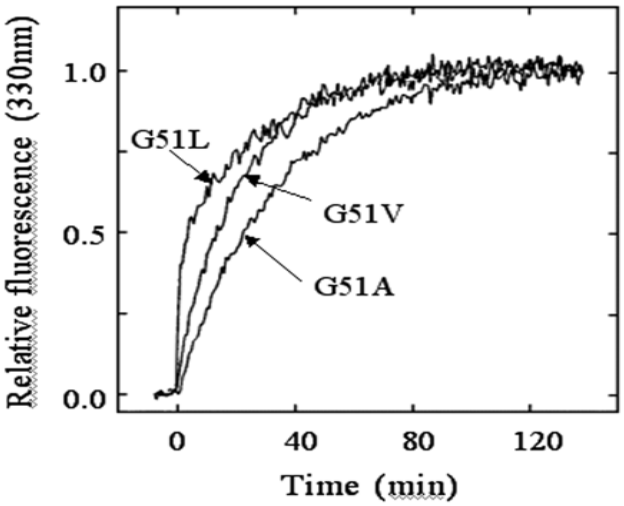

Fig. IV.1.3. Fluorescence MetaII decay of the Wt and the Gly-51 mutants. The fluorescence MetaII decay assays were carried out in buffer A. All data are the average of two different experiments.

Rhodopsin	$t^{1/2}$[a] retinal release in buffer A min	$t^{1/2}$ retinal release in G_t assay buffer min	Fluorescence G_t activation *Relative initial rates*[b]
Wt	14.2	12.7	1.00
G51A	23.2	18.7	0.95
G51V	15.4	1.9 (39%) 30.2 (61%)	0.20
G51L	0.7 (36%) 19.8 (64%)	0.8 (38%) 22.0 (62%)	0.00
G89A	11.8	9.6	1.02
G89L	12.4	9.2	0.68
G89F	13.5	10.8	1.22
G89K	12.7	10.2	0.62
G89D	29.1	2.9 (18%) 38.5 (82%)	0.57

Table IV.1.3. $t^{1/2}$ life times for retinal release and G_t activation for the Wt and mutant rhodopsins. [a] $t^{1/2}$ values for the retinal release were measured using fluorescence spectroscopy. [b] G_t activation was measured using fluorescence spectroscopy. The fluorescence values were obtained from the fitting of the data points from the first 60s of the curve and normalized to the Wt value. All values are the average of duplicate experiments

Regarding the ability of these mutants to function normally in signal transduction, G51A could activate G_t to essentially the same level as Wt. Mutant G51V, however, showed a very reduced level of G_t activation, which was dependent on the time after bleaching when the protein was added to the G_t reaction mixture (Figure IV.1.4B). When the G51V mutant was added to the reaction mixture immediately after bleaching (time 0 in Figure IV.1.4B), the maximum activation corresponded to an initial rate about 0.2 that of Wt (maximal G_t activation for this mutant, 100% in Figure IV.1.4B). When the bleached G51V protein was added after several minutes, the initial rate of the G_t activation was reduced, and after 12min it was essentially abolished. The curve obtained in Figure IV.1.4B has a $t^{1/2}$ of about 2min, which correlates nicely with the $t^{1/2}$ of the fast component of the fluorescence Meta II decay in G_t assay buffer. The G51L mutant did not show any significant degree of activation under any experimental conditions, even upon addition of the protein immediately after bleaching.

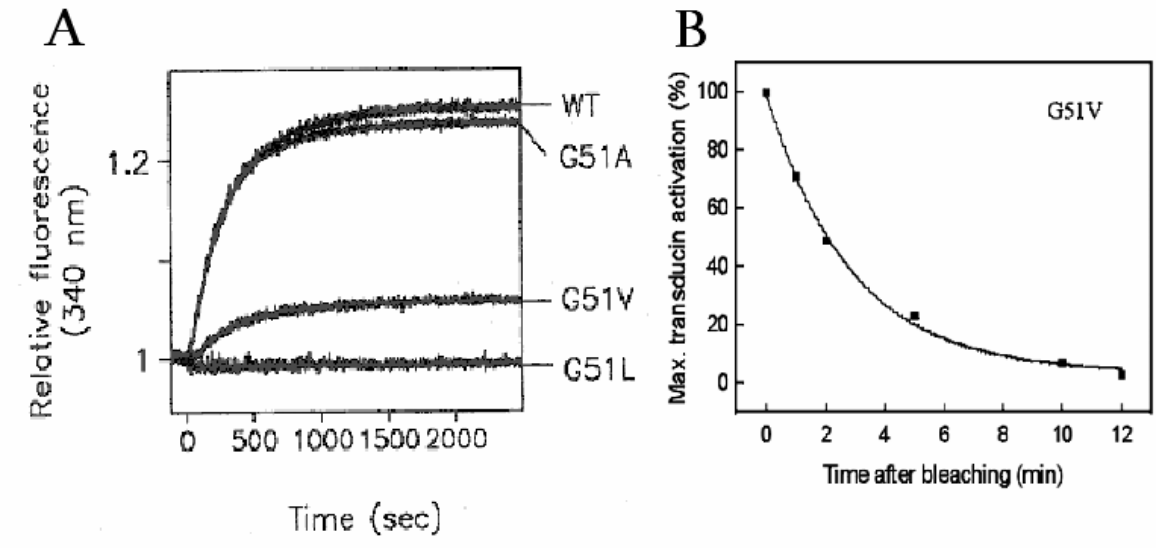

FIG. IV.1.4. A. Relative G_t activation of Gly-51 mutants. B. G_t activation of G51V mutant at different times after bleaching. G_t initial rates were plotted for reactions started at different times after bleaching of the mutant protein sample. All data are the average of two different experiments. Temperature, 20 °C.

IV.1.3. EXPRESSION AND CHARACTERIZATION OF MUTATIONS AT POSITION 89 IN HELIX II

Several mutants at position 89, the site of the naturally occurring G89D mutation, were constructed, expressed, and characterized. The mutants studied were G89A, G89L, G89F, G89K, and G89D. The mutant proteins were expressed at similar levels to that of Wt in the case of the hydrophobic replacements G89A, G89L, and G89F. Replacements where an ionizable, presumably charged side chain was introduced (G89K and G89D) were expressed at a much lower level, about one-fifth that of the Wt. The electrophoretic pattern for the correctly folded fraction of these mutants was Wt-like, with the main opsin band at 40kDa and the characteristic trailing smear (not shown).

UV-visible absorption spectra of the mutant proteins eluted in buffer A showed A_{280}/A_{500} ratios of 1.6–1.8 (Figure IV.1.2). It should be noted that G89A, G89L, and G89F could form chromophore to a similar extent as Wt upon elution in phosphate-buffered saline, pH 7.2. The substitutions involving an ionizable amino acid side chain had significantly higher A_{280}/A_{500} ratios, in the 2.5–2.8 range, indicating that they were eluted as mixtures of folded

and misfolded proteins. The separated folded fractions showed A_{280}/A_{500} ratios of 1.7–1.8 (Figure IV.1.2). UV-visible absorption spectrum in the dark, corresponding to the G89K mutant, showed a clear definite UV-absorbing band centered at 350nm in addition to the normal chromophoric band at 500nm. All the other mutants showed a Wt-like band in the visible region at 500nm, and no wavelength shifts were detected.

The MetaII decay of G89A, G89L, G89F, and G89K was slightly faster than the Wt in normal assay conditions. In the G_t assay buffer the decays for these mutants were only slightly faster when compared with the values obtained in buffer A. G89D showed a different behavior in this assay. Its decay in buffer A was slow with a $t_{1/2}$ of 29.1min (single exponential fit); but in G_t assay buffer the fluorescence curve was best fit to a double exponential function, with a fast component ($t_{1/2}$, 2.9min) and a slow component ($t_{1/2}$, 38.5min) (Table IV.1.II). This behavior, specific to the adRP G89D mutant, was not seen in any other of the mutants at position 89.

G_t activation of mutant G89A was similar to that of Wt. G89F showed a higher initial rate of G_t activation, whereas G89L had about 30% reduction in the rate. The two mutants that showed lower G_t activation were G89K and G89D. In particular, the G89D mutant rhodopsin, associated with adRP, showed more than a 50% reduction in the initial G_t activation rate (Figure IV.1.5 and Table IV.1.III).

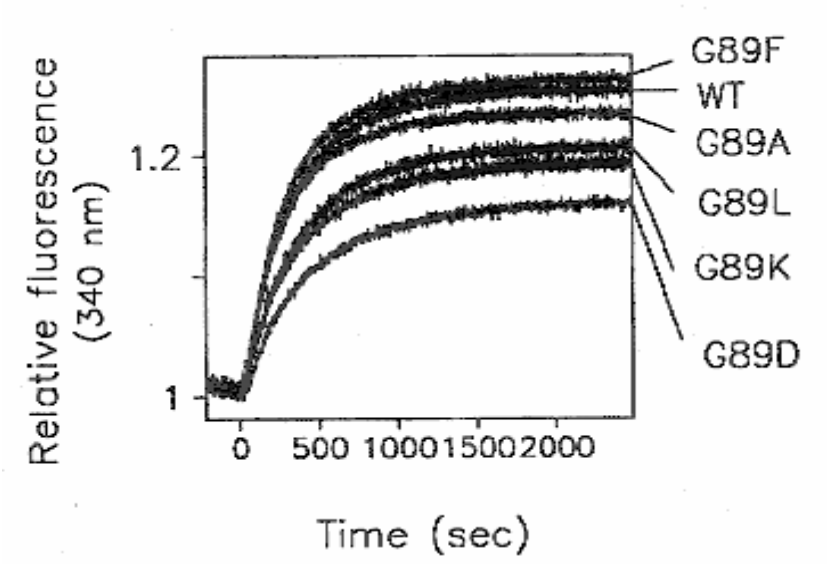

Fig.IV.1.5. Relative G_t activation of Wt and Gly-89 mutants.

IV.1.4. DISCUSION

Mutations at Position 51 in Helix I—Gly-51 in the transmembrane helix I of rhodopsin is part of a G*XXX*N motif conserved in the GPCR superfamily. The naturally occurring mutations G51A and G51V are found in adRP patients. It was reported that conservative mutations in the transmembrane region of rhodopsin cause misfolding of the mutant proteins [Garriga et al., 1996]. However, in those cases that the mutant proteins are able to form the correct retinal binding pocket, it is intriguing as to why they are still deleterious. We constructed and expressed the synthetic G51L mutant to explore the effect of the size of the amino acid side chain in the packing of the helices and in signal transduction.

The correctly folded fractions of the mutant rhodopsins were separated and characterized. The folded fractions of the three mutants gave UV-visible absorption spectra with A_{280}/A_{500} ratios of 1.6–1.7. The SDS-PAGE pattern was like that for the Wt protein with no lower bands, characteristic of mutants with altered phenotype. Although these features would point to mutants having a similar phenotype to that of the Wt, other parameters studied indicate that these mutant proteins are destabilized, both thermally, in the dark, and also after photo-activation, when compared with Wt. The mutant proteins in the dark are less stable than Wt, with the stability decreasing with increasing size of the side chain. A number of factors are shown to affect the thermal stability of dark-state rhodopsin, including retinal disease-causing mutations [Ramon et al., 2003a] or zinc binding [del Valle et al., 2003]. Other factors mediating the stability of dark-state rhodopsin are proposed, like a conserved ion-pair interaction in the intradiscal loop E-II of rhodopsin [Janz et al., 2003]. A destabilizing effect is also observed for the active intermediate MetaII of the Gly-51 mutants formed upon photobleaching. The decrease in the ability of the mutants to activate G_t can also be correlated with the increase in size of the side chain at position 51 and point to a disruption of the interhelical packing due to the mutations. The fact that an increase in one or two carbon atoms makes such a significant difference indicates a tight steric coupling with another amino acid side chain. From the reported crystal structure [Palczewski et al., 2000], this interact ion is probably with Val-300 in transmembrane helix VII (Figure IV.1.6A). The substitution of glycine at position 51 by the bulkier valine and leucine side chains would result in steric clash with the Val-300 side chain (Figure IV.1.6, B and C) and perturbation of the local helical environment of Pro-303 (involved in the pronounced kink

of helix VII) included in the conserved NP*XXY* motif of the GPCR superfamily. This motif or amino acids within it are thought to be important in receptor signaling [Gales et al., 2002, Gripentrog et al., 2000, Govaerts et al., 2001, Prioleau et al., 2002, Fritze et al., 2003]. For example, interaction between Met-257 in helix VI and this motif has been suggested in the case of rhodopsin from a site-directed mutagenesis study [Han et al., 1998].

It is noted that for G51V there is a relationship between the time after bleaching and the ability of the mutant protein to activate G_t. Mutation to alanine in the G51A mutant can be tolerated, but G51V and G51L show a clearly altered behavior upon illumination and are clearly defective in signal transduction. The impaired ability of these mutants to activate G_t is, thus, correlated with the decreased stability of the active conformation MetaII. That was also the case in the C110A/C187A double mutant that could form chromophore but had a destabilized MetaII species [Davidson et al., 1994].

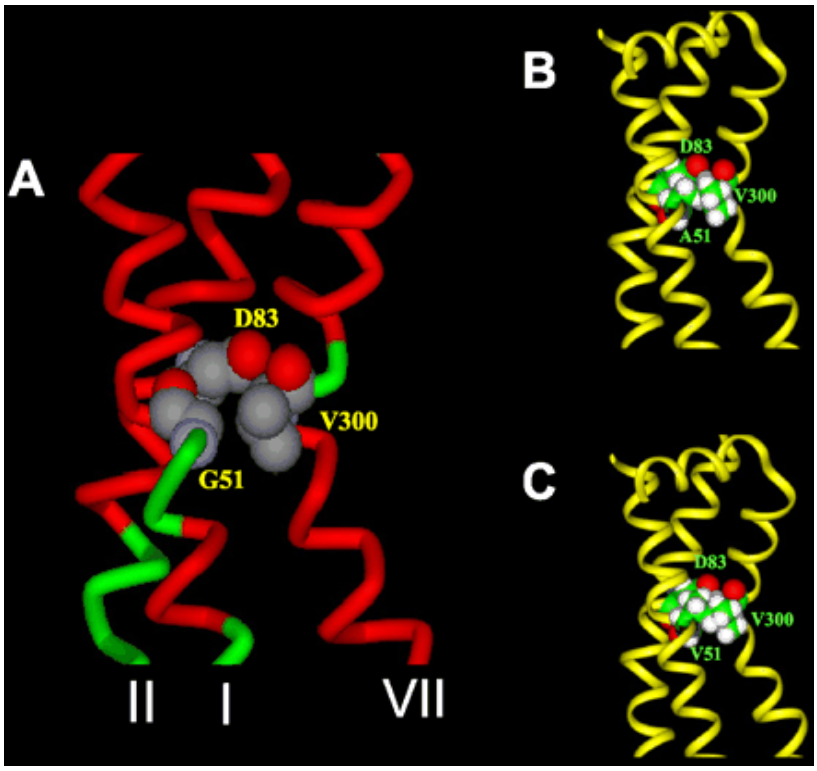

Fig.IV.1.6. **Model of helices I, II, and VII of rhodopsin.** Model in the region of interest around G51 showing helices I, II, and VII. This model is based on the coordinates from 1L9H PDB [Okada et al., 2002]. *A*, model for the Wt with native G51. The proximity of G51 in helix I and Val-300 in helix VII can be observed. The proximity of Asp-83 in helix II to Val-300 (coming from behind) is also shown. This model was generated with the program DS ViewerPro (Accelrys Inc.). *B*, model for mutant G51A with the introduced alanine coming closer to Val-300 in helix VII. *C*, model for mutant G51V (adRP). Note the increased contact between Val-51 and Val-300. The models in *B* and *C* were prepared using Insight II (Accelrys Inc.). In these models the eighth cytoplasmic helix after the region of Val-300 in helix VII is shown. This helix is known to be important in G_t activation. Mutation at Gly-51 would perturb interaction with Val-300 in helix VII, and this change could be transmitted to the cytoplasmic helix 8, thus affecting G_t activation.

Fluorescence MetaII decay results can be best fit to double exponential functions, reflecting a fast component and a slow component (Table IV.1.III). These double exponential curves could be explained by assuming that two different species with different kinetics are formed. Thus, in the case of the mutants reported, the fluorescence increase observed could be interpreted as reflecting the direct decay of MetaII to free all-*trans*-retinal and formation of a non-active rhodopsin conformation that could be the MetaIII species [Heck et al., 2003]. The fast MetaII decay correlates with the G_t activation values obtained for mutants G51V and G51L (Figure IV.1.4A and Table IV.1.III). The decrease in the G_t activation rate at different times after bleaching obtained for mutant G51V has a $t^{1/2}$ of about 2 min for the process, which correlates with the $t^{1/2}$ for the fast component of the fluorescence decay curve (in G_t assay buffer), proposed to reflect decay to opsin and all-*trans*-retinal.

Mutations at Position 89 in Helix II—In this case the size of the side chain does not seem to be as important as the charge of the introduced side chain. Of all the mutants at this position, only the G89D mutant rhodopsin had abnormal photobleaching [Hwa et al., 1997]. This mutant also showed a slow rate for retinal release, in agreement with previous studies [Hwa et al., 1997]. However the G89D mutant in G_t assay buffer showed the biphasic behavior observed for the G51V and G51L mutants. Gly-89 is next to Gly-90 in transmembrane helix II. The G90D mutant is associated with the retinal disease CSNB, and the aspartate in the mutant would be in the retinal binding pocket next to the Schiff base [Rao et al., 1994]. In the same region, another mutation related to congenital night blindness, T94I, is reported to have very unusual thermal and conformational properties [Ramon et al., 2003a]. Gly-89 forms a cavity together with Gly-90, and a water molecule is located very close to the carbonyl group of Gly-89 at hydrogen-bonding distance [Okada et al., 2002]. A functional role for the water molecules associated to rhodopsin has been recently proposed [Okada et al., 2002]. In this regard, the Gly-89 to Lys mutation, which also decreases the rate of G_t activation, may disrupt the Gly-89-water interaction and perturb a fine electrostatic network in the vicinity of the retinal Schiff base. In the case of G89K, this mutant showed a UV-absorbing species at about 350nm in the absorption spectrum in the dark, which was not previously observed in any other mutant studied so far. This species corresponds to a Schiff base-linked chromophore because it shifts to 440nm upon acidification of the sample (not shown). Interestingly, *Drosophila* UV pigments have

lysine at a homologous position in the Gly-89/Gly-90 region in human rhodopsin [Fryxell and Meyerowitz, 1987, Alkorta and Du, 1994]. A lysine in the second transmembrane helix of the invertebrate UV pigments was proposed to affect wavelength regulation via a charge interaction [Gartner and Towner, 1995].

For the other mutations, G89A shows similar G_t activation to the Wt. However, G89F and G89L show opposite effects; G89F slightly increases the activity, whereas G89L decreases it. Because phenylalanine is a bulky residue, the observed difference in activation may be related to the stereochemistry of the side chains, planar for Phe *versus* tetrahedral for Leu rather than to the actual molar volume of the corresponding side chains.

Structural Consequences of Mutations at Gly-51 and Gly-89—We have shown that position 51 in helix I of rhodopsin is very sensitive to the size of the introduced side chain. The G51V mutant associated with adRP is defective in signal transduction and has an unstable MetaII active conformation. For mutations at position 89 (located closer to the retinal Schiff base), although some role can be assigned to the size of the side chain, the results obtained for G89D and G89K suggest that charge effect is more important for mutations at this position. The other mutation associated with adRP, G89D, is also shown to be defective in signal transduction. Transmembrane helix II was not previously implicated in conformational rearrangements (involving helix movements) during the G_t activation process. However, very recently a structural change in helix II of the angiotensin II type 1 receptor has been reported [Miura and Karnik, 2002]. Furthermore, the interaction between helix II and helix VII has also been postulated [Miura et al., 2003]. In rhodopsin, the highly conserved Asp-83 in helix II is close to Val-300 in helix VII and may be hydrogen-bonded to the amide nitrogen of this amino acid through a water molecule [Okada et al., 2002]. Mutations at position 89, although in a region closer to the retinal Schiff base than to the Gly-51 region, could cause a helical rearrangement that would result in changes at Asp-83 in the same helix, disrupting the interaction with Val-300 in helix VII. A model showing the proximity of Gly-51 in helix I, Val-300 in helix VII, and Asp-83 in helix II is shown in Figure IV.1.6. Our results indicate that helix I and helix II are important in the stability and function of rhodopsin and suggest a novel interplay between these helices and helix VII in the structure and in the conformational rearrangements ensuing photoactivation of rhodopsin.

Physiological Relevance with Regard to RP—Mutations G51A, G51V, and G89D have been found in RP patients and cause retinal degeneration. Because of extreme genetic and clinical heterogeneity of RP [Farrar et al., 2002] it is difficult to correlate the molecular defect caused by a given mutation in rhodopsin and the severity of RP. Despite this heterogeneity, an effort was made to correlate the disease progression in patients with adRP and rhodopsin mutations [Berson et al., 2002]. In this study, clinical features regarding patients with G51V and G89D mutations are presented [Berson et al., 2002]. These data indicate that G51V mutation results in a more benign clinical phenotype than G89D. G89D is especially defective in electroretinogram amplitude (indicating significant loss of retinal function). Our biochemical and spectroscopic data show that these two mutants show altered photobleaching and altered functionality. The two mutants show biphasic retinal release curves with a significant amount of the slow component being formed that may be interpreted as reflecting formation of non-active species. Interestingly, mutant G89D, which shows a more severe clinical phenotype than G51V [Berson et al., 2002], shows a higher amount of this slow species formed (82% for the former compared with 61% for the latter). In the case of mutants G51A and G89D, these were reported to be partially misfolded [Hwa et al., 1997]. However, in the study of the folded fraction of the G51A mutant reported here the only difference observed with regard to the Wt properties is its reduced thermal stability in the dark. Unfortunately no clinical data are available for this mutant. The results obtained for G51V and G89D mutants associated with adDP suggest that in addition to a structural effect, reduced stability and subsequent failure in G_t activation can also have implications in RP caused by mutations in rhodopsin.